Dynamics of the Neuronal Intermediate Filaments

Shigeo Okabe, Hiroshi Miyasaka, and Nobutaka Hirokawa

Department of Anatomy and Cell Biology, School of Medicine, University of Tokyo, Hongo, Tokyo, 113 Japan

Abstract. We have analyzed the dynamics of neuronal intermediate filaments in living neurons by using the method of photobleaching of fluorescently-labeled neurofilament L protein and immunoelectron microscopy of incorporation sites of biotinylated neurofilament L protein. Low-light-level imaging and photobleaching of growing axons of mouse sensory neurons did not affect the rate of either axonal growth or the addition of intermediate filament structures at the axon terminal, suggesting that any perturbations caused by these optical methods would be minimal. After laser photobleaching, recovery of fluorescence did occur slowly with a recovery half-time of 40 min. Furthermore, we observed a more rapid fluorescence recovery in growing axons than in quiescent ones, indicating a growth-dependent regulation of the turnover rate. Incorporation sites of biotin-labeled neurofilament L protein were localized as numerous discrete sites along the axon, and they slowly elongated to become continuous arrays 24 h after injection. Collectively, these results indicate that neuronal intermediate filaments in growing axons turn over within the small area of the axoplasm possibly by the mechanism of lateral and segmental incorporation of new subunits.

THE cytoskeleton of nerve cells is composed of three classes of polymers: microtubules (MTs),[1] actin filaments, and neurofilaments (NFs). Neurofilaments belong to a heterogeneous type of intermediate filaments (IFs), which are composed of distinct subunit proteins expressed in a tissue-specific and developmentally regulated manner (Franke, 1987; Steinert et al., 1985). Although previous biochemical and structural studies have shown that NFs are the major framework of mammalian neurons after maturation (Hoffman and Lasek, 1975; Schlaepfer and Lynch, 1977; Shaw and Weber, 1981; Hirokawa et al., 1984; Hirokawa, 1982, 1991), the molecular mechanism of the dynamic exchange of NF proteins in neurons and their interactions with other cytoskeletal elements are not well known in comparison with MTs and actin filaments. Because IFs including NFs have poor solubility in physiological buffers and because the unpolymerized pool of IF proteins is thought to be very small (Soellner et al., 1985), the idea has prevailed that IFs are polymerized instantaneously after translation to become a totally static structure. However, there is now increasing evidence to suggest that a continuous turnover of IFs is involved in maintaining the IF structure and function in living cells. The first line of evidence on the dynamic nature of IFs is from experiments using the forced expression of IF genes in cultured cells. Transfection of native and mutated IF genes has revealed the successive incorporation of newly synthesized IF proteins into pre-existing IF networks (Albers and Fuchs, 1987; Chin and Liem, 1989; Monterio and Cleveland, 1989; Ngai et al., 1990) and also the disruption of endogenous IF networks by the integration of assembly-incompetent mutant proteins (Lu and Lane, 1990; McCormick et al., 1990; Wang and Cleveland, 1990). A second experimental approach is based on the technique of introducing chemically modified IF proteins into living cells, which has been applied successfully in monitoring the dynamics of other cytoskeletal proteins in vivo. Biotin-labeled vimentin or keratin introduced by the aid of microinjection technique was progressively incorporated into endogenous IF networks, suggesting a possible pool of soluble IF subunits undergoing exchange with polymerized IFs (Vikstrom et al., 1989; Miller et al., 1991). These results collectively indicate that a continuous incorporation of subunits into the polymerized IFs does occur and is possibly required for the maintenance of this filament system.

The growing evidence on the dynamic nature of IF networks in vivo has raised a possibility that NFs are not a totally static structure and soluble subunits or oligomers can be the unit of the axonal transport (Hollenbeck, 1989; Nixon, 1992). Indeed, recent analyses using the introduction of biotin or fluorescently labeled tubulin or actin into living neurons and successive immunoelectron microscopy or photobleaching have shown that the other two axonal cytoskeletal polymers, MTs and actin filaments, are dynamic structures, emphasizing the possible role of dynamic exchange between soluble and polymerized cytoskeletal proteins in the formation and maintenance of the axonal cytoskeleton (Okabe and Hirokawa, 1988, 1989, 1990, 1991). In addition,

1. *Abbreviations used in this paper*: DRG, dorsal root ganglia; IF, intermediate filament; MT, microtubule; NF, neurofilament; NF-L, neurofilament L protein.

this view has gained support from the recently developed technique of photoactivation of caged-fluorescein labeled MTs, which also shed light on the anterograde translocation of MTs in rapidly growing *Xenopus* axons, a unique feature of this neuron type (Reinsch et al., 1991; Okabe and Hirokawa, 1992). This active exchange of subunits in MT and actin filament systems in the axon, together with the recent findings that other intermediate filament systems are dynamic, leads to the expectation that reversible polymerization and subunit exchange of the NF system in neurons may be directly visualized by techniques of molecular cytochemistry, which includes biotin-mediated immunocytochemistry, photobleaching of fluorescent probes and photoactivation of caged-fluorescein labeled probes.

To monitor the dynamics of NFs in vivo, we produced fluorescent and biotinylated analogues of neurofilament L protein (NF-L) by labeling NF-L at a cysteine residue, and introduced it into living neurons. Photobleaching of fluorescently labeled NF-L and immunoelectron microscopic analysis of the incorporation sites of biotin-labeled NF-L suggested that NFs are a dynamic structure which turn over within a small region of the axoplasm by exchanging subunits at discrete sites on the filaments.

Materials and Methods

Preparation of Fluorescein- or Biotin-labeled NF-L Protein

NF-L protein was purified from bovine spinal cord according to the method of Geisler and Weber (1981) with slight modifications (Hisanaga and Hirokawa, 1988). Polymerized NF-L in an assembly buffer (20 mM Pipes, pH 6.8, 1 mM EGTA, 1 mM $MgCl_2$, 170 mM NaCl) was treated with 1 mM DTT to reduce cysteine residue. After centrifugation, the sample was dissolved in 6 M urea buffer (6 M urea, 10 mM sodium phosphate, pH 7.5, 0.5 mM EGTA, 0.1 mM EDTA, 1 mM $MgCl_2$) and passed through a Sephadex G-25 column which had been equilibrated with 6 M urea buffer. The fractions containing NF-L protein were combined, adjusted to the protein concentration of 2–5 mg/ml, and reacted with either 5'-iodoacetoamido fluorescein (Molecular Probes Inc., Junction City, OR) or maleimidobutyryl biocytin (Calbiochem-Behring Corp., San Diego, CA) at a molar ratio of 1:20 for 1 h at 20°C. The reaction was stopped by the addition of DTT to the final concentration of 1 mM. Unbound dye was separated on a Sephadex G-25 column and the fractions containing labeled NF-L protein were collected and dialyzed overnight against an assembly buffer to form filaments. Polymerized NF-L was collected by centrifugation, dissolved in 6 M urea buffer, clarified by centrifugation, and then dialyzed against a low-salt buffer (5 mM Hepes, pH 8.5, 0.1 mM EGTA, 0.1 mM EDTA, 0.1 mM DTT) for 6–8 h. NF-L was shown to remain soluble in a low-salt buffer and this preparation was clarified by centrifugation and then used for microinjection at the concentration of 5–8 mg/ml. When the labeled sample had to be stored before microinjection, labeled NF-L polymerized by dialysis against an assembly buffer was frozen as small aliquots in liquid N_2.

Microinjection of Labeled NF-L Proteins

Microinjection was performed as previously described (Okabe and Hirokawa, 1988). Because the formation of filament aggregates at the tip of the microneedle blocks the sample flow, the tip was filled with a small amount of distilled water and the sample containing labeled NF-L was backfilled. During the period of distilled water out flow, the out-flow rate was precisely adjusted to prevent a blockage at the tip of the needle. This method greatly facilitated the microinjection into living cells.

Cell Culture

BSC1 cells were grown in MEM (Gibco Laboratories, Grand Island, NY) containing 15 mM Hepes, pH 7.4, and 5% FCS. COS cells were maintained in RPMI medium (Gibco Laboratories) supplemented with 10% FCS. Preparation of DRG neurons from young adult mice was done as previously described (Okabe and Hirokawa, 1990). Cells were plated onto poly-L-lysine coated coverslips and incubated overnight without NGF. Under this condition (i.e., on less adhesive substrate without NGF), DRG neurons remained without neurites or with only sprouting neurites 8–12 h after plating. Microinjection was done at this time point and NGF was added to the medium at a concentration of 50 ng/ml. At 12–24 h after the addition of NGF (24–36 h after plating), the neurite elongation rate reached the maximal value under this culture condition. However, the growth rate at this time point (<30 μm/h) was less than that with more adhesive substrates such as laminin (10–80 μm/h) (Okabe and Hirokawa, 1992).

Low-light-level Imaging and Photobleaching of Fluorescent NF-L

Fluorescent imaging was done using an Olympus IMT-2 inverted microscope and a Nikon X100 fluor objective lens (1.3 NA). 50 W halogen lamps were used for both *trans*- and epi-illumination. For phase-contrast observation at higher magnification, a handmade phase-contrast ring was inserted at the front plane of the condenser. Images were projected to an image intensifier coupled with a CCD camera (C2400-87, Hamamatsu Photonics, Hamamatsu, Japan). For fluorescence images, the ICCD camera was set at the maximum gain and the epi-illumination halogen lamp was used at ~2/3 intensity. For phase images, the gain of the ICCD camera was at the minimum. Video frames were summed and averaged for 1 s, and background fluorescence was subtracted with a digital image processor (Hamamatsu Photonics, ARGUS-100). Images were stored on tape using an SP.U-matic video cassette recorder (model VO-9600, SONY, Tokyo, Japan). The condition of photobleaching was described in detail previously (Okabe and Hirokawa, 1993). Briefly, using an argon ion laser (GLS-3050, NEC, Tokyo, Japan) operated at minimum output and a cylindrical lens, the cross-section of a beam in the specimen plane was a bar with a peak intensity of 2.7 MW/m^2 and a half-width of 3.3 μm at 1/10 intensity. This focused beam was applied for 1/30 s to provide a total energy of 0.09 MJ/m^2, resulting in a reduction of the fluorescence intensity of fluorescein labeled NF-L to 20–50% of the initial value (see Fig. 10). The fact that total bleaching of fluorescence did not occur under this bleaching condition must be emphasized.

Immunofluorescence

For staining of BSC1 and COS cells injected with fluorescein- or biotin-labeled NF-L, cells were fixed with 2% paraformaldehyde in PBS for 20 min, treated with 0.2% Triton X-100 in PBS for 15 min, and then exposed to 10% normal goat serum in PBS for 30 min. For cells injected with biotin NF-L, the samples were reacted successively with polyclonal anti-biotin antibody (Enzo Biochem, Inc., New York, NY), fluorescein-conjugated goat anti-rabbit IgG, monoclonal anti-vimentin (Amersham Corp., Arlington Heights, IL), and rhodamine-conjugated goat anti-mouse IgG. For cells injected with fluorescein labeled NF-L, the step of biotin staining was omitted.

For immuno-detection of NF-L, M, and H in DRG neurons, cells were fixed with −20°C chilled methanol for 6 min, incubated with 3% normal goat serum in PBS for 30 min, and then treated with 0.1% Triton X-100 in PBS for 10 min. The samples were then reacted with mouse monoclonal antibodies to either NF-L (Boehringer Mannheim Diagnostics Inc., Houston, TX), NF-M or NF-H (Biomakor, Rehovot, Israel), and then with fluorescein-conjugated goat anti-mouse IgG.

Immunoelectron Microscopy

Cells were washed with PBS, permeabilized with PHEM buffer (60 mM Pipes, 25 mM Hepes, 10 mM EGTA, and 2 mM $MgCl_2$, pH 6.9) plus 0.2% Triton X-100 and 10 μM taxol for 2 min at 37°C, and then fixed with 0.3% glutaraldehyde in PHEM buffer for 30 min. The method of immunolabeling with biotin, embedding and sectioning was as previously described (Okabe and Hirokawa, 1988; 1991).

Detergent Extraction of Fluorescein-labeled NF-L Injected into DRG Neurons

Neurons containing fluorescein-labeled NF-L were illuminated under identical conditions before and after detergent extraction. Images were projected to an SIT camera (C2400-08, Hamamatsu Photonics) coupled to an image processor (ARGUS-100, Hamamatsu Photonics) and all quantifications

were done on digitized images. In the intensity range used for the fluorescence image detection, the SIT camera output was linear. After acquisition of the fluorescence image of living neurons, cells were first washed with PHEM buffer, and then permeabilized with 0.02% saponin in PHEM buffer for 5 min. The image of the permeabilized neurons was obtained immediately after the detergent treatment. All procedures were performed on the microscope stage without moving the sample from the image field.

Image Analysis

Production of the intensity profiles of photobleached axons was done as previously described (Okabe and Hirokawa, 1991). Quantification of the fluorescence intensity in the bleached spot was performed by setting a rectangle on the bleached spot and calculating the average of pixel intensities within the rectangle for each frame. Background fluorescence was subtracted for each frame by setting a rectangle of the same shape on the specimen plane where no fluorescent objects existed. In the intensity range of the fluorescence images, the ICCD camera was linear on its output.

In Vitro Photobleaching of Fluorescein-labeled NF-L

To observe fluorescent NFs in vitro, fluorescein-labeled NF-L was dialyzed against an assembly buffer to form filaments, diluted with the same buffer to 50 μg/ml and absorbed onto the formvar film supported by locator grids. The grid was placed in a drop of the assembly buffer on a coverslip and illuminated by the same optical system used for the photobleaching of neurons except that a cylindrical lens was omitted to produce a beam spot of the larger diameter. After bleaching with different doses at several positions of the same grid, the sample was negatively stained and observed in an electron microscope.

Other Methods

Rhodamine-labeled BSA was prepared as previously described (Okabe and Hirokawa, 1991). NF-L subunit was polymerized by dialysis against the reassembly buffer of 0.17 M NaCl, 20 mM Pipes, pH 6.8, 1 mM $MgCl_2$, 1 mM EGTA, 1 mM DTT at 37°C for 3 h and negatively stained with 1% uranyl acetate.

Results

Characterization of Fluorescein- and Biotin-labeled NF-L

The presence of only one cysteine residue in the primary structure of NF-L protein (Geisler et al., 1985; Lewis and Cowan, 1985) suggests that the labeling stoichiometry of 1:1 would be easily accomplished by reacting NF-L as a dissociated molecule in the presence of 6 M urea. As expected, NF-L was able to be labeled rapidly with 5′-iodoacetoamido fluorescein, a sulfhydryl-specific labeling agent, at the molar f-to-p ratio of 1:1. This finding was consistent with a previous report of Angelides et al. (1989), where labeling of NF-L with another sulfhydryl-specific agent, fluorescein-5-maleimide, was presented. Fig. 1 *A* (lanes *1*, *2*) shows SDS-PAGE of fluorescein-labeled NF-L. At the end of the purification, there was no detectable free dye associated with NF-L. The labeling of NF-L with maleimidobutyryl biocytin was done under conditions identical to those for 5′-iodoacetoamido fluorescein. Fig. 1 *A* (lane *3*) shows SDS-PAGE of biotin-labeled NF-L. Negative-stain electron microscopy of fluorescein- or biotin-labeled NF-L protein dialyzed against reassembly buffer shows the formation of smooth-walled filaments, which were morphologically indistinguishable from native neurofilaments (Fig. 1, *B* and *C*).

To confirm that fluorescein- and biotin-labeled NF-L can be incorporated in vivo into the IF network, we microinjected these probes into cultured fibroblasts. Because our previous study showed that NF-L protein remained soluble in a low-salt solution at alkaline pH (Hisanaga and Hirokawa, 1990), fluorescein- or biotin-labeled NF-L protein was first disassembled in urea buffer, dialyzed against a low-salt solution at alkaline pH, clarified by centrifugation and then used for microinjection. Soon after injection, fluorescein- or biotin-labeled NF-L formed aggregates of various sizes near the nucleus. Within 4–12 h after injection, the aggregates gradually disappeared and were replaced by a network which had a similar appearance to the endogenous vimentin network. After 12–24 h, the localization of fluorescein- or biotin-labeled NF-L was almost identical with that of endogenous vimentin filaments (Fig. 1, *D–G*). These results indicate that exogenously introduced NF-L, which belongs to Class 4 IFs, can form co-polymers with a Class 3 IF protein, vimentin. This is consistent with recent transfection experiments using cDNA of NF-L, where the incorporation of newly synthesized NF protein into the pre-existing vimentin network of fibroblasts was observed (Chin and Liem, 1989; Monterio and Cleveland, 1989). Although the observed time course of incorporation into the IF network is likely to be rather slow compared with that of biotin-vimentin (Vikstrom et al., 1989) or biotin-keratin (Miller et al., 1991), we did not attempt to further characterize the pattern of NF-L incorporation into the fibroblastic IF network.

Incorporation of NF-L into the Cytoskeleton of Mouse Sensory Neurons

As a model system for axonal growth, we have used a primary culture of mouse sensory neurons. Previous studies indicated that there are mainly two neuronal populations in dorsal root ganglia (DRG): one consists of large diameter cells immunoreactive with NF triplet proteins and the other of small diameter ones containing peripherin (Lawson et al., 1984; Parysek and Goldman, 1988). Consistent with these previous reports, large diameter neurons isolated from mouse DRG were immunoreactive with all neurofilament triplet proteins (Fig. 2). We first injected rhodamine-labeled BSA into large sensory neurons in culture and stained them with anti-NF-L protein. Almost all (>95%) of the injected neurons were stained with anti-NF-L, indicating that selective injection into NF-containing sensory neurons is possible. In the following experiments, we analyzed only large diameter neurons in culture, which presumably contain NFs as a component of the IF network.

To ensure the total incorporation of injected labeled NF-L protein into the native IF network of DRG neurons, we introduced labeled NF-L into DRG neurons with no neurites or with only sprouting neurites 8–12 h after plating. After microinjection, NGF was added to the medium to facilitate neurite elongation, and the cells which contained long extending neurites were further processed for photobleaching 12–24 h after injection (that is, 24–36 h after plating). To see whether fluorescein-labeled NF-L is fully incorporated into IF system of DRG axons, we quantified fluorescence intensity before and after detergent treatment of the axon of neurons which had been injected with fluorescein-labeled NF-L. As shown in Fig. 3 *A* and *B*, most of the fluorescein signal remained after extraction of soluble proteins by detergent treatment under conditions where rhodamine-BSA was completely extracted (Fig. 3, *C* and *D*). From five different experimental runs, the fluorescent signal remained after detergent extraction was calculated to be 90.6 ± 8.5 (±SEM)%

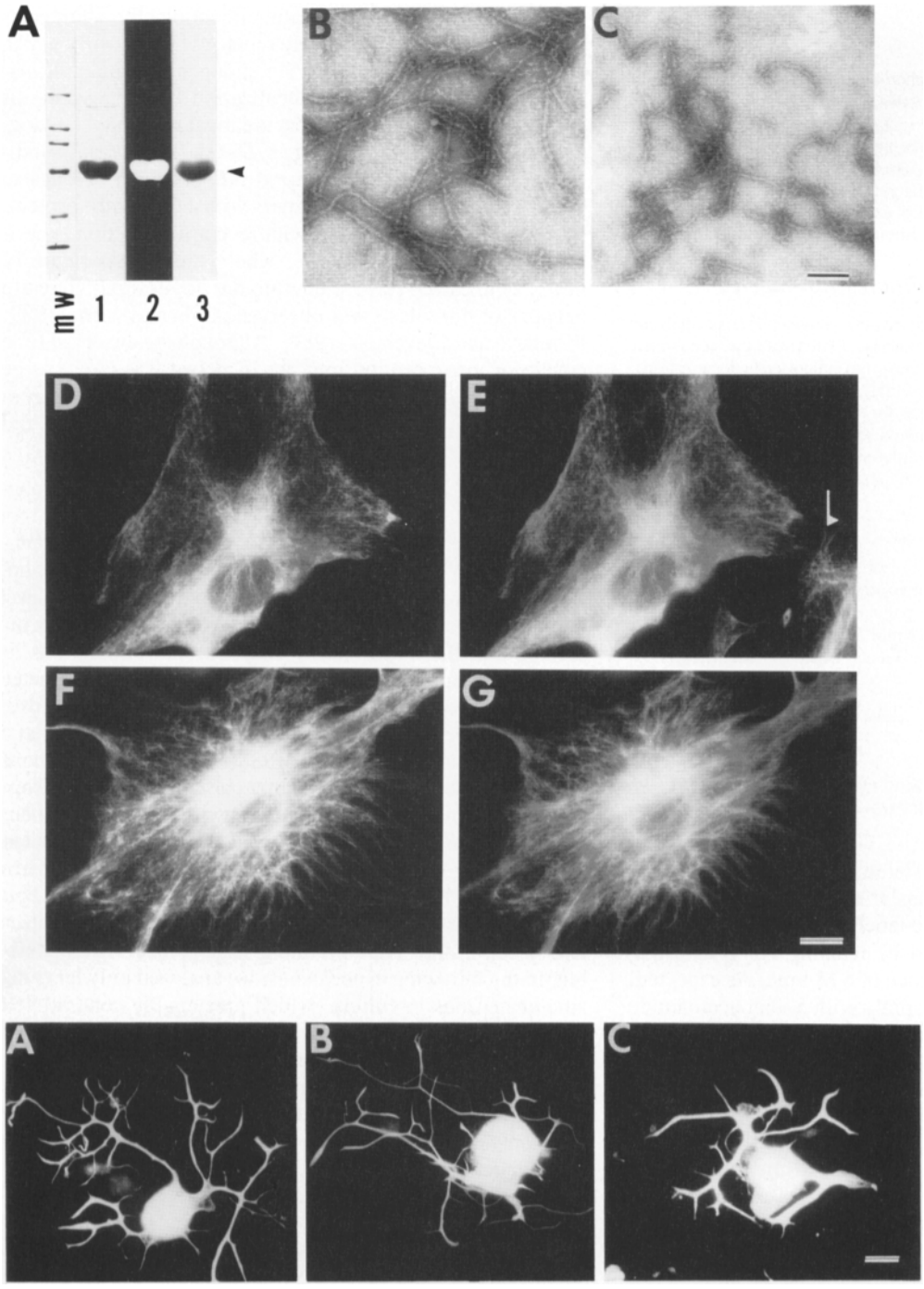

Figure 1. Characterization of fluorescein- or biotin-labeled NF-L. (*A*) SDS-polyacrylamide gel analysis of the preparation of fluorescein- or biotin-labeled NF-L. Fluorescein-labeled NF-L (lanes *1* and *2*) and biotin-labeled NF-L (lane *3*) were analyzed by dye staining (lanes *1* and *3*) or by UV illumination (lane *2*). The samples contain a single band of 68-kD polypeptides (*arrowhead*). (mw) Molecular weight standards, from top to bottom, 200, 116, 92, 66, 43, and 31 kD. (*B* and *C*) Negative-stain electron micrographs of fluorescein- (*B*) and biotin-labeled (*C*) NF-L. Smooth-walled filaments can be observed. Bar, 100 nm. (*D* and *E*) A BSC-1 fibroblast injected with fluorescein-labeled NF-L and fixed 12 h after injection. Cells were processed for indirect immunofluorescence with antivimentin and rhodamine-conjugated secondary antibody. The fibrous pattern of fluorescein-labeled NF-L (*D*) is largely identical with the anti-vimentin staining (*E*). Arrow indicates an uninjected cell, which can be detected only with rhodamine channel. (*F* and *G*) A COS fibroblastic cell injected with biotin-NF-L and fixed 16 h after injection. Cells were processed for double-label indirect immunofluorescence using an anti-biotin antibody (*F*) and an anti-vimentin antibody (*G*). The staining pattern is almost identical. Bar, 10 μm.

Figure 2. Immunofluorescence micrographs of large DRG neurons reacted with anti-NF-L (*A*), anti-NF-M (*B*), and anti-NF-H (*C*) antibodies. Cell bodies and neurites strongly reacted with all antibodies. Bar, 10 μm.

of initial fluorescence intensity. Although 5(6)-carboxyfluorescein fluorescence is pH dependent, its intensity is near maximal at physiological pH (~7.0) and at pH of the extraction buffer (~6.8), because the pKa for the deprotonation of 5(6)-carboxy-fluorescein is 6.4-6.5 (Tsien, 1989). For this reason, we think that the effect of the pH change during extraction would be minimal for fluorescence intensity measurements. The small amount of fluorescent signal solubilized by detergent extraction indicates that a large part of the injected NF-L protein has been incorporated into the insoluble fraction of DRG neurons 12 h after injection.

Photobleaching of Fluorescent NFs in Mouse DRG Axons

To determine the dynamics of NFs in the axon, we bleached

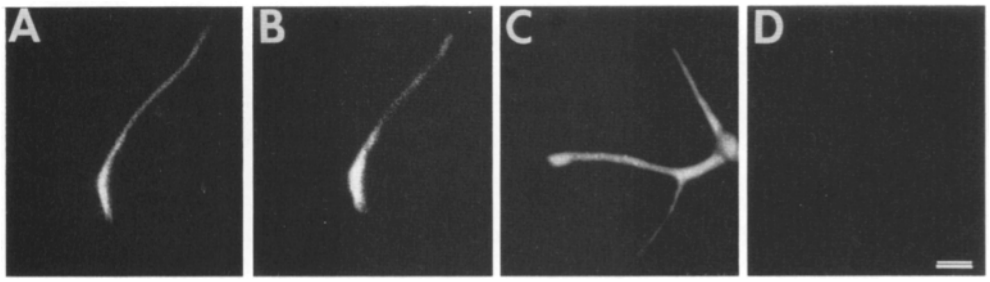

Figure 3. Extraction of fluorescent derivatives microinjected into DRG neurons. DRG neurons were injected with fluorescein-labeled NF-L (*A* and *B*) or rhodamine-labeled BSA (*C* and *D*) 12 h before extraction experiments. Fluorescence images were taken just before (*A* and *C*) and after (*B* and *D*) extraction. Fluorescein-labeled NF-L remained in the detergent insoluble fraction under the condition where rhodamine-BSA is largely extracted. Bar, 10 μm.

a small region of the axon containing fluorescein-labeled NF-L and analyzed the fluorescence recovery by using low-light-level video microscopy of living neurons. For this kind of experimental approach to faithfully reveal the dynamic nature of fluorescent molecules, it is essential to ensure that neither the intense pulse light for laser photobleaching nor the attenuated blue light for epi-illumination disturbs the biological processes.

We first determined whether there was any structural damage on NF structures in photobleached regions in vitro by negative-stain EM. The laser beam illuminated circular areas with a 69-μm diam at the light intensity of which peak value was 0.59 MW/m² on the formvar film supported by locator grids. Fluorescently labeled NFs were polymerized in vitro, absorbed on the grids, and several areas on a single grid were bleached with a series of exposure times ranging from 0.5–8.0 s, corresponding to the total laser energy of 0.3–4.7 MJ/m². After bleaching, grids were incubated for 2–30 min before staining by uranyl acetate and then observed in an electron microscope. By this method, we could observe the effect of photobleaching with various exposure times under the same condition of the sample preparation and negative staining. When fluorescent NF-L was illuminated at 4.7 MJ/m², the fragmentation of NF-L was evident (Fig. 4 *C*), and the illumination area also tended to be positively stained. In contrast, structure of fluorescent NFs was almost identical to that in the control area on the same grid regardless of the incubation time after bleaching when the total energy was <1.2 MJ/m². These results indicate that the structural damage of NFs due to photobleaching occurs at the energy range similar to the value reported to cause dissolution of fluorescent MTs in vitro (Okabe and Hirokawa, 1993) and we chose the total energy of 0.1 MJ/m² for the following photobleaching experiments on cultured neurons.

We next determined whether there was any detectable change in NF arrays in photobleached regions by immunostaining with anti-NF antibody. The total energy was set to 0.1 MJ/m² and beam profile and exposure time were identical to the conditions we employed to monitor MT dynamics in neurons (Okabe and Hirokawa, 1990, 1993). The photobleached neurons were fixed at various times ranging from 2 to 60 min after photobleaching and were stained with anti-NF-L or NF-M antibodies. NF arrays were intact in photobleached regions at least on a light microscopic level regardless of the time that had elapsed since they were bleached (Fig. 5), indicating that the fluorophore can be bleached without disrupting NF arrays. We also investigated the effect of photobleaching on a wider zone along the neurite. If bleached zones can be set to be >30 μm, we could expect to see the pattern of incorporation of new subunits into this wide window. However, we found that the breakage of NF structure became more evident as the bleached zones were set to be wider, and it was difficult to make clear bleached zones without causing any breakage of NFs when the width of the bleached zone was set to be >20 μm. This dependency of photodamage on the total area of illumination was not evident in experiments in vitro, but similar correlation was also observed in the experiments of photobleaching fluorescent MTs in living mouse neurons. We suspect that this positive correlation between photodamage and the total area of illumination in vivo is related to the higher accumulation of oxygen radicals in the axoplasm by intense laser light compared with the in vitro situation where oxygen radicals can diffuse more rapidly.

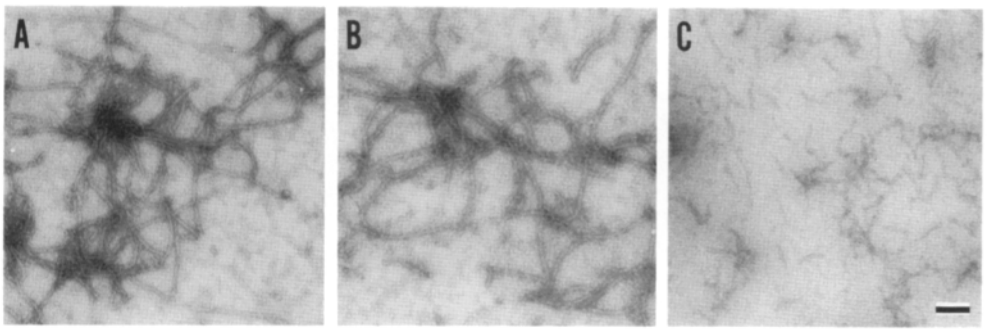

Figure 4. In vitro photobleaching of NHS-FL labeled NF-L. Fluorescent NF-L was polymerized in vitro, bleached with a laser beam, and then observed by negative stain electron microscopy. The regions, where 488 nm light at the total energy of 0 (*A*), 1.2 (*B*), and 4.7 (*C*) MJ/m² were applied, are presented. Bar, 100 nm.

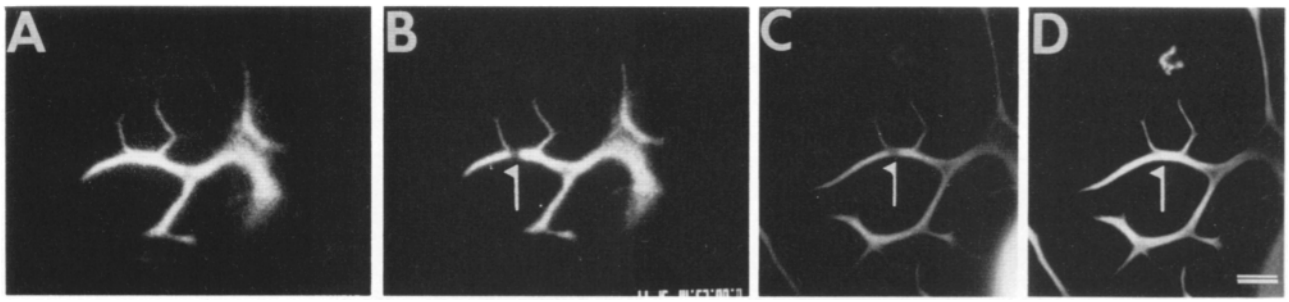

Figure 5. Fluorescence micrographs of a DRG neuron before and after photobleaching. Images of a living neurite containing fluorescein-labeled NF-L were taken before (*A*) and after (*B*) photobleaching, and then the cell was fixed 10 min after bleaching (*C*). The cell was processed for indirect immunofluorescence using an anti-NF-L antibody (*D*), showing that NFs in the bleached zone were intact (*B–D, arrows*). Bar, 10 μm.

To detect the possible effects of successive exposures with a weak light source for epi-illumination, 10 or more frames of the images of growing fluorescent axons were taken at short intervals of 10–20 min. Fig. 6 shows a time lapse sequence of fluorescent and phase images of a growing axon. No inhibition of axonal growth was detected, and the progressive formation of NF arrays at the distal end of the axon was observed. These observations suggest that the period of exposure for the image acquisition had little effect on axonal growth and formation of the NF structure in the axon. Interestingly, the distal end of the growing axon was devoid of fluorescence in all image pairs. This further supports that there was total incorporation of fluorescein-labeled NF-L into the cytoskeleton, and also revealed a delay in the assembly of the IF structure relative to the advance of the axon tip.

It is still possible that the combination of laser photobleaching and sequential image acquisition by epi-illumination affects the dynamics of the NF system. However, when photobleaching was performed in the middle of the sequential acquisition of fluorescent images, no retardation in the progressive growth of NF arrays in the axon was observed (Fig. 7). Furthermore, the absence of the beading of neurites, a normal activity of growth cones, and the lack of any disturbance of organelle transport across the bleached zone suggest the absence of perturbation.

We observed a gradual increase of the fluorescent signal in the bleached zone with time (Figs. 7, 8). To quantify the turnover rate, we produced intensity profiles of the digital images, calculated the total intensity in the bleached regions, and estimated the recovery half-time from the plot of the total intensity in the bleached zones against time (Fig. 9, *A* and *B*). From these plots, the recovery half-time was calculated to be 40.6 ± 4.0 (±SEM) min ($n = 25$), suggesting that NFs turn over within the small area of the axoplasm. Comparison of the fluorescence recovery of both growing and quiescent axons (see Figs. 7 and 8) pointed to the possible dependence of the rate of recovery on the rate of neurite growth. To test this possibility, we divided the experimental runs into the following categories. (*a*) Neurites with growing tips. Elongation of neurites at the rate of >10 μm/h was observed during the period of 1 h after photobleaching. (*b*) Neurites without growing tips. Elongation of neurites was <10 μm/h. As shown in Fig. 9 *C*, fluorescence recovery was slower in the quiescent neurites (46.2 ± 6.2 min; $n = 14$) than in the growing neurites (27.9 ± 4.1 min; $n = 10$).

In contrast, the difference in the rate of fluorescence recovery was less significant when the experimental runs were divided into groups according to the position of photobleaching (Fig. 9 *C*). When we further subdivided growing tip and stem from nongrowing tip and stem, the difference between the tip and stem was also not prominent compared with the difference between growing and nongrowing ones (Fig. 9 *C*). These results indicate that the turnover of NFs is regulated in a growth-dependent manner and that the spatial difference is rather small.

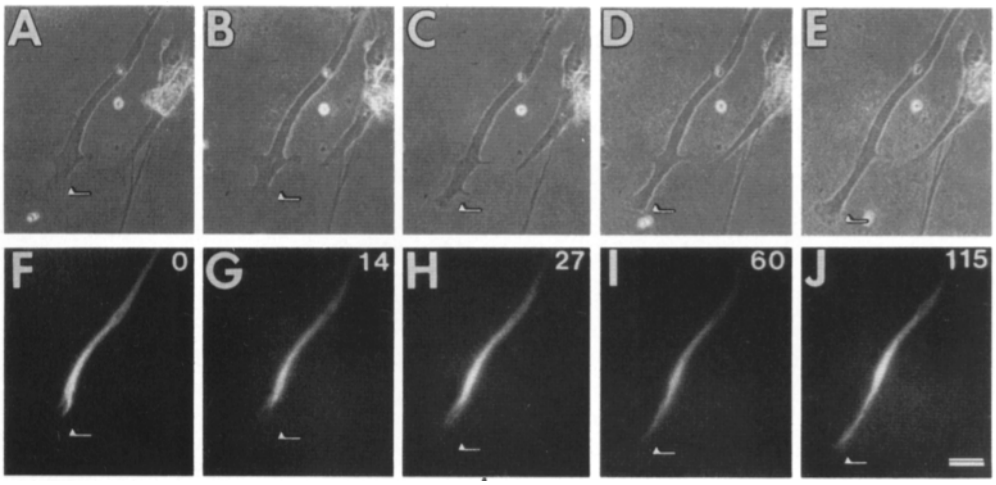

Figure 6. Neurite growth and formation of the NF structure during observation of fluorescent images of NFs. Phase contrast (*A–E*) and fluorescence (*F–J*) images were collected at time points presented in the upper right-hand corners of *F–J*. The distal end of the growing axon is indicated by arrows. The fluorescent NF structure does not reach the distal end of the axon (*F–J, arrows*). Progressive formation of the fluorscent NF structure is observed (*F–J*). Bar, 10 μm.

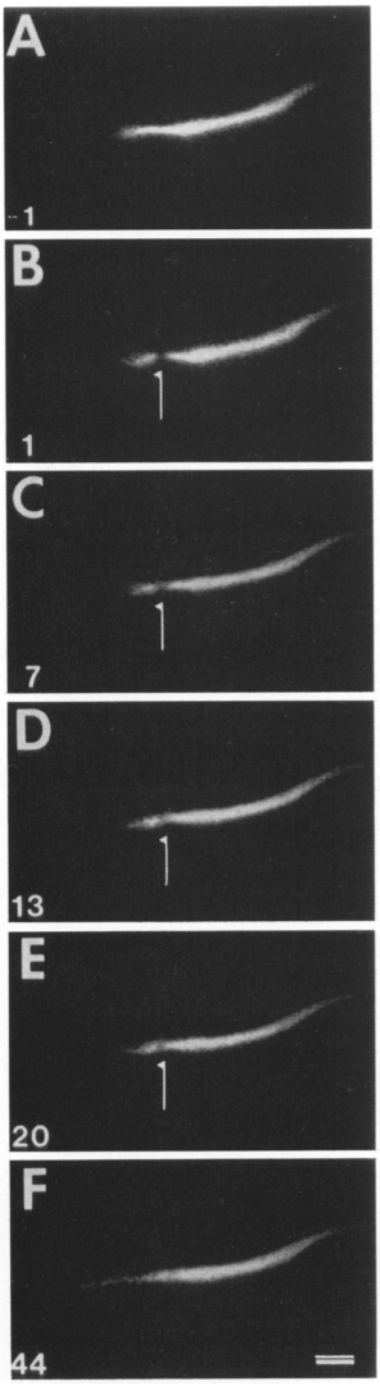

Figure 7. Photobleaching of fluorescent NFs in the growing neurite of a mouse DRG neuron. A narrow zone was photobleached with a laser pulse (*B*, *arrow*) and fluorescence recovery was monitored by recording images of fluorescein-labeled NF-L intermittently. Times in minutes relative to the photobleaching pulse are shown in the lower left-hand corner of each panel. Bar, 10 μm.

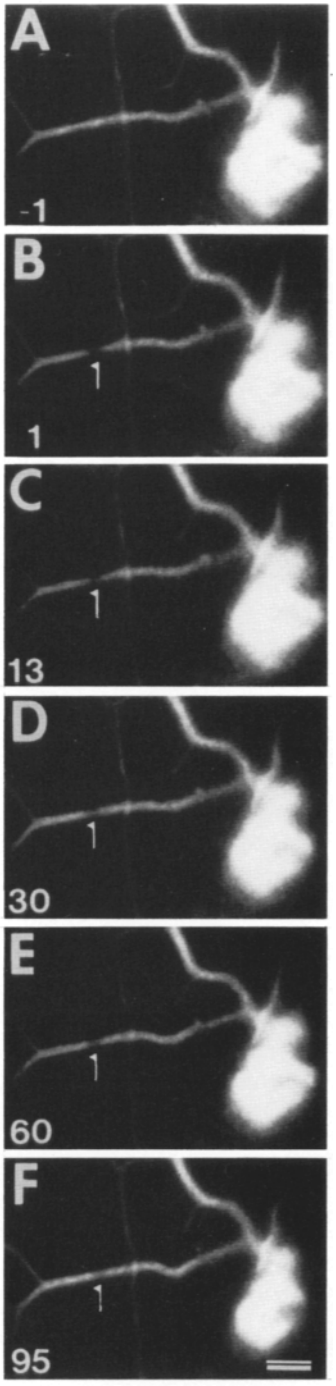

Figure 8. Photobleaching run in a quiescent neurite of a mouse DRG neuron. Fluorescent images of photobleached NFs were recorded intermittently. Gradual recovery of fluorescence was observed (*arrows*). Elapsed time (min) after photobleaching is shown in the lower left-hand corner of each panel. Bar, 10 μm.

Because the turnover of fluorescence was more rapid in growing axons and the neurite extension was slow on polylysine-coated coverslips, it was generally difficult to determine whether the translocation of bleached spots occurred or not during the period of significant axonal elongation. However, in some photobleaching runs on growing axons where fluorescence recovery was slow, we were able to trace the position of bleached spots until a detectable increase of the axonal structure and NF arrays distal to the bleached zone did occur. As shown in Fig. 10, we observed no anterograde movement of photobleached spots during the period of significant neurite elongation. This was confirmed by creating the fluorescence intensity profiles in Fig. 10 *K*, which show no vectorial movement of the trough with time. Of total 25 photobleaching runs, no movement of bleached zone during neurite elongation was observed in four cases. In other cases, whether net increase of IF structure did occur or not was difficult to judge. These results suggest that NF-L protein necessary for constructing NF arrays at the distal end of the axon can be transported across the bleached spot which is stationary and turns over within a local region of the axoplasm.

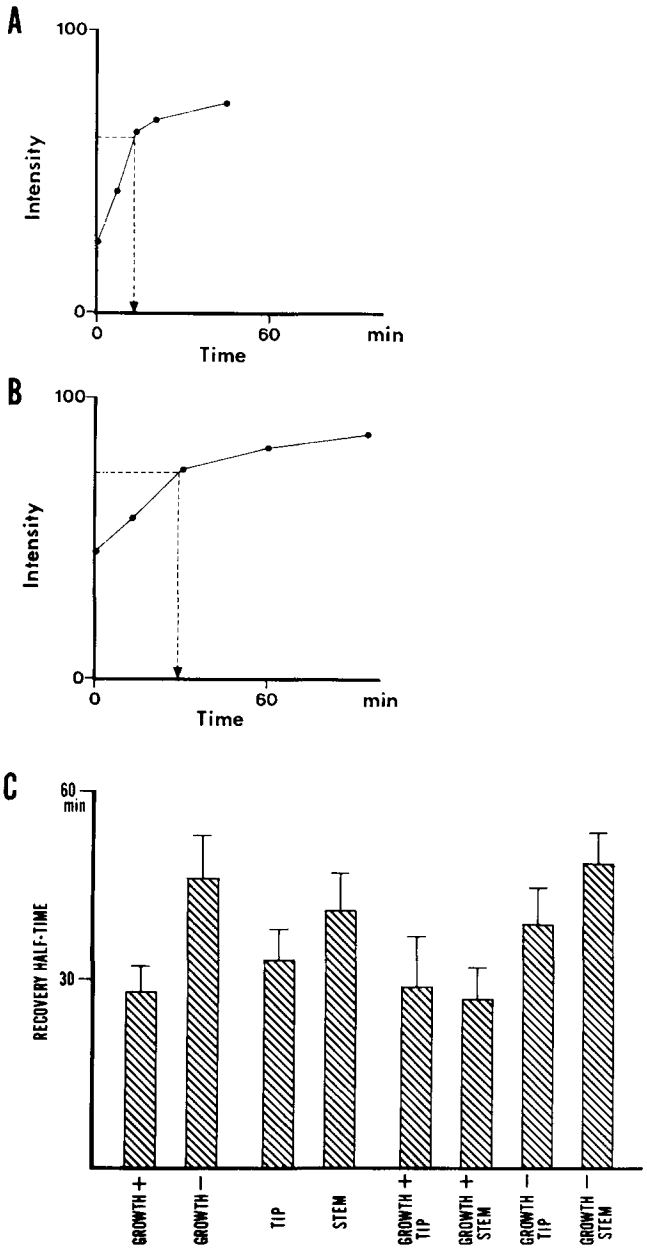

Figure 9. Quantification of fluorescence recovery after photobleaching. (*A* and *B*) Fluorescence intensities in the bleached regions were plotted against time for the neurites shown in Figs. 7 and 8. The recovery half-time was determined from these plots (*arrows*) to be 13 min (*A*) and 29 min (*B*). (*C*) Recovery half-time of fluorescence within the bleached region. Fluorescence recovery half-time was 27.0 ± 4.1 min (n = 10) for growing neurites, 46.2 ± 6.2 min (n = 14) for quiescent neurites, 32.4 ± 5.6 min (n = 8) for the bleached zone located within 50 μm from the neurite tip and 41.1 ± 6.0 min (n = 16) for the bleached zone >50 μm from the neurite tip.

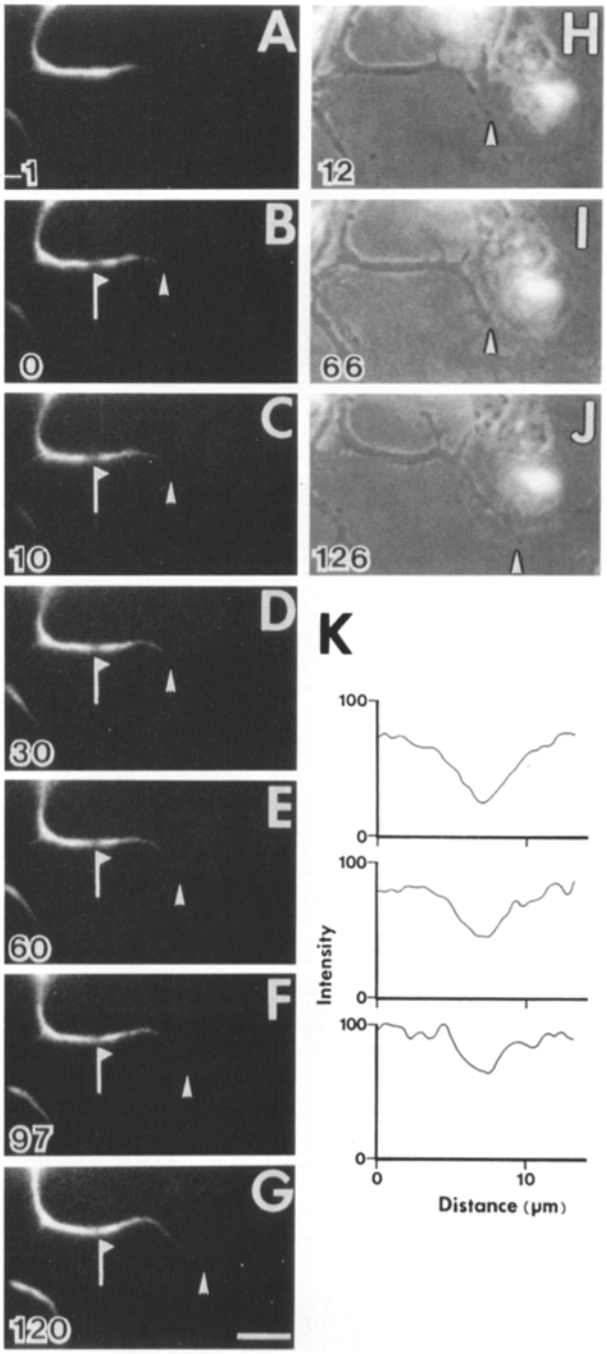

Figure 10. Photobleaching run in a growing neurite of a mouse DRG neuron. (*A–G*) Fluorescent images of a growing neurite containing fluorescein-labeled NF-L. The bleached zone did not move during the observation (*arrows*), while growth of the fluorescent NFs distal to the bleached zone was observed (*arrowheads*). Elapsed time after photobleaching is shown in the lower left-hand corner of each panel. (*H–J*) Phase contrast images of the growing neurite during observation. Advancement of the neurite tip is indicated by arrowheads. (*K*) Intensity profiles of fluorescence across the bleached zone. No anterograde movement of the trough was observed. Time point of each profile is as follows: from top to bottom, 12 s (Fig. 10 *B*), 30 min 19 s (Fig. 10 *D*), 120 min 40 s (Fig. 10 *G*). Bar, 10 μm.

Immunoelectron Microscopic Analysis of Incorporation of Biotin-NF-L into the Axonal Cytoskeleton

To analyze the sites of NF-L protein incorporation into the axonal cytoskeleton, we microinjected biotin-labeled NF-L into DRG neurons 2 d after plating. At this time point, DRG neurons had already extended the length of their neurites by as much as 500 μm. When the overall pattern of biotin-NF-L incorporation was monitored by immunofluorescence microscopy of detergent extracted cells at various times after injection, the incorporation of biotin-labeled NF-L along the length of the neurites was observed 12–24 h after injection. Therefore, we performed immunoelectron microscopic ob-

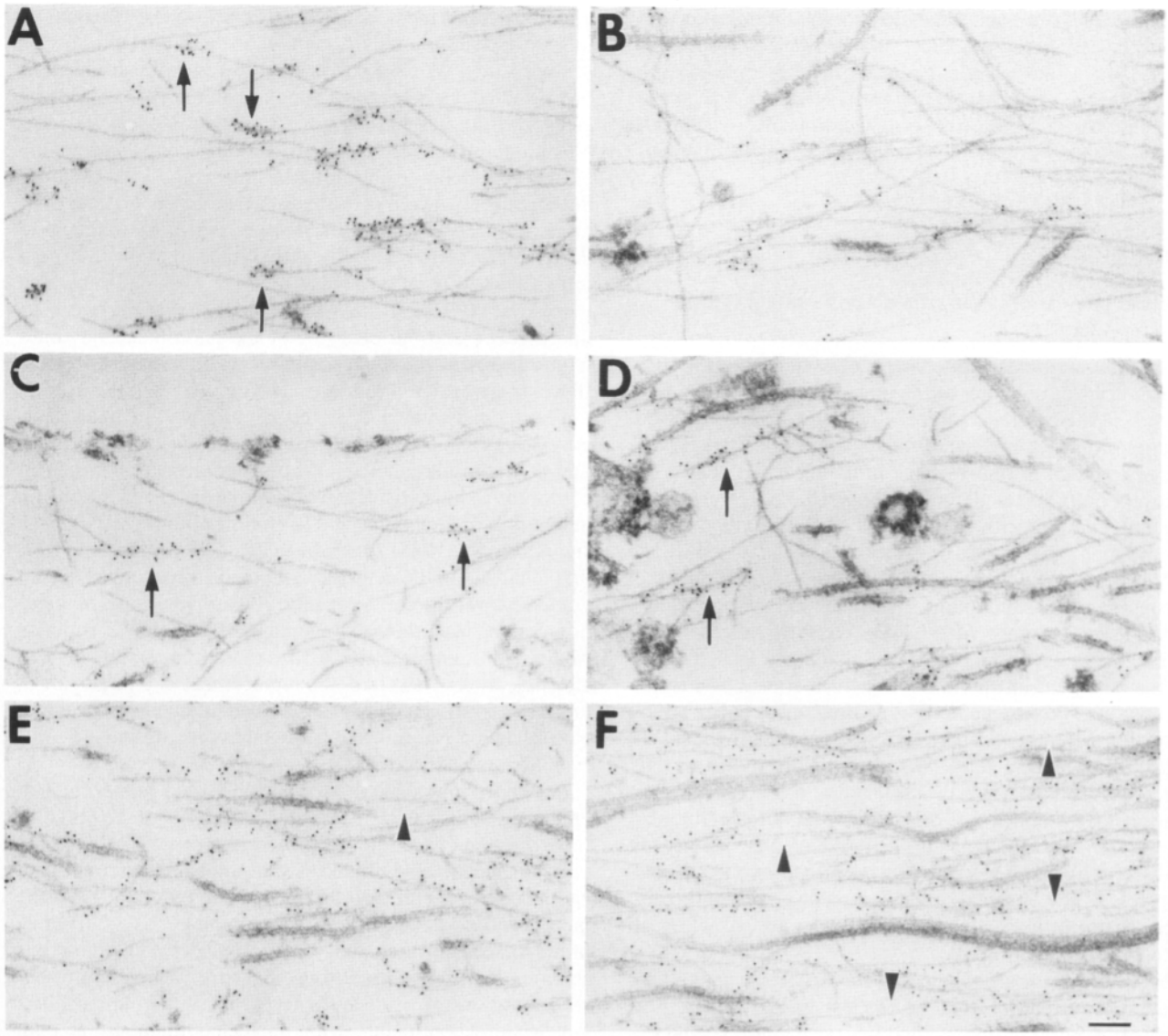

Figure 11. Immunoelectron microscopy of DRG neurons injected with biotin-labeled NF-L. (*A*) Cell body of a DRG neuron permeabilized and fixed 1 h after injection. IF segments which are heavily decorated with colloidal gold particles are continuous to unlabeled segments (*arrows*). (*B*) A region of a neurite which is 100–200 μm away from the cell body shown in (*A*). A few gold particles are associated with IFs but do not form distinct segments. (*C* and *D*) Regions of neurites which are located 100–200 μm away from the cell body. The cell was permeabilized and fixed 3 h after injection. IF segments, decorated with gold particles and continuous with unlabeled segments, were observed (*arrows*). (*E* and *F*) Neurites of cells permeabilized and fixed 22 h after injection. The images were from regions 100–200 μm away from cell bodies. More homogeneous labeling of IFs in the neurites was observed. However, IF segments completely devoid of gold particles were also present (*arrowheads*). Bar, 100 nm.

servations on DRG neurons permeabilized and fixed 1, 3, and 22 h after injection. At each time point, 3–5 cells which had no detectable damage due to microinjection were processed for immunoelectron microscopy.

IFs in the cell body were found to be labeled with antibiotin antibody 1 h after injection, but very few gold particles were seen on the filaments in the axons >100 μm away from the cell body. IFs in the cell body were labeled densely at discrete foci, which were randomly distributed both at the terminal and middle portions of single filaments, suggesting the location of possible incorporation sites along their lengths (Fig. 11 *A*, *arrows*). No dense nucleation of biotin-NF-L from the nucleus was detected. In the axons of cells fixed 1 h after injection, we observed a few gold particles associated with IFs (Fig. 11 *B*). Because the concentration of gold particles was greater than in uninjected cells processed in an identical fashion, it is likely that the association of 2–3 gold particles with IFs reflects the incorporation site of biotin-NF-L molecules.

At 3 h after injection, more gold particles were observed to be associated with IFs in the axon (*arrows*, Fig. 11 *C* and *D*). Compared with the axon of 1 h incubation, the region along single IFs decorated with gold particles had elongated significantly, suggesting continuous incorporation of biotin-labeled NF-L at discrete sites along neuronal IFs. We observed no bulk replacement of IF arrays by newly formed IFs at the proximal part of the axon, meaning that this analysis found no evidence of bulk movement of IFs toward the axon tip. At 22 h after injection, IFs were more homogeneously labeled with antibiotin (Fig. 11, *E* and *F*). However, as there

were IFs which were still unlabeled with antibiotin (Fig. 11, *E* and *F*, *arrowheads*), this suggested that the complete turnover of IFs was not yet accomplished. The gradual elongation of the NF segments which exchanged subunits in the axon indicates that the turnover of neuronal IFs occurs locally by the mechanism of replacement of single filaments from discrete foci.

Discussion

Turnover of Neuronal Intermediate Filaments in Growing Axons

In this study we presented two items of evidence for the continuous turnover of neuronal IFs in growing axons. The first evidence of the dynamic nature of neuronal IFs was derived from photobleaching experiments which revealed the gradual recovery of fluorescence in the bleached zone with a recovery half-time of 40 min. Although the photobleaching technique is a powerful approach, the interpretation of the data depends on whether fluorescent probes function normally in vivo and whether the irradiation for bleaching the fluorophore is harmless for living samples. Fluorescein-labeled NF-L protein formed IFs in vitro, formed copolymers with vimentin in fibroblasts, and was incorporated into the detergent-insoluble fraction 12 h after introduction into neurons. Taken together with a previous report characterizing the assembly properties of fluorescein-labeled NF-L in vitro (Angelides et al., 1989), these results indicated that fluorescein-labeled NF-L protein can be used as a reliable probe on NF dynamics in vivo. Direct observation of fluorescent NF-L in growing axons also revealed the ability of fluorescein-labeled NF-L to be incorporated into the axonal IF arrays, as the absence of a fluorescent signal in the advancing axon tip indicates the largely assembled nature of fluorescent probes in the axon shaft.

There have been arguments on the possible effects of irradiation from photobleaching (Vigers et al., 1988). The ability of photobleaching method has been controversial especially in regard to the MT system, because the recently developed technique of photoactivation of caged-fluorescein labeled tubulin has provided a different picture of MT dynamics in both mitotic cells and in neurons (Gorbsky et al., 1988; Mitchison, 1989; Okabe and Hirokawa, 1990; Lim et al., 1990; Reinsch et al., 1991). The discrepancy between photobleaching and photoactivation studies on mitotic cells could be largely explained by the fact that the photobleached mark on mitotic spindles is rapidly recovered by soluble tubulin subunits and nonkinetochore MTs, whereas the photoactivated mark on slowly exchanging kinetochore MTs persists longer (Mitchison, 1989). In the case of axonal MTs, where soluble tubulin subunits and subunit exchanges are much fewer, the divergent behavior of photobleached and photoactivated marks was somewhat of an enigma (Reinsch et al., 1991). However, we very recently reported that this discrepancy is likely to be derived from different mechanical properties of mouse and *Xenopus* axons in culture (Okabe and Hirokawa, 1992). Furthermore, photobleaching experiments on growing *Xenopus* neurons have revealed anterograde movement of photobleached MTs (Okabe and Hirokawa, 1993).

So far, recent photoactivation and photobleaching efforts on the axons of different species strongly suggest that the photobleaching method is able to disclose the behavior of MTs as accurately as the photoactivation method. In the present study, we have carried out a series of examinations on the effect of photobleaching, including ultrastructural analysis of fluorescent NFs in vitro, immunolocalization of NFs in the bleached zone at various time points and tracing of the advancing axon tip after bleaching. In addition, fluorescent NFs were partially bleached to 20–50% of their initial fluorescence using irradiation conditions identical to those employed to reveal the anterograde movement of photobleached MTs in growing *Xenopus* axons (Okabe and Hirokawa, 1993). Thus, we think that the recovery of fluorescence and the behavior of the photobleached zones faithfully reveal the dynamic properties of the endogenous IF networks in DRG neurons.

The second evidence of the IF turnover in neurons is provided by the electron microscopic analysis of incorporation sites of biotin-labeled NF-L. Major artifacts of these "incorporation sites" arise from injection trauma and the abrupt increase of free subunit concentration within cells (Okabe and Hirokawa, 1988). Because injected biotin-labeled NF-L first localized in the cell body and then spread into the axon gradually over the course of several hours, the effect of injection trauma and transient increase of free NF-L subunits would be minimum in the distal axon at time points of >1 h after injection. Therefore, the replacement of a large part of the IF network by newly assembled filaments containing biotin-labeled NF-L strongly suggests the continuous turnover of axonal IF arrays.

Incorporation of biotin-labeled NF-L into numerous discrete sites along the IF arrays is consistent with the previous report of Ngai et al. (1990), where the expression of avian vimentin gene was initiated within mouse cells containing endogenous vimentin by dexamethasone induction, and the incorporation of avian vimentin polypeptide was observed by immunoelectron microscopy to be restricted to numerous spots on the vimentin network. Because we frequently observed regions of IFs heavily decorated with gold particles, which were continuous with unlabeled filaments at both ends, the incorporation is not likely to be restricted to filament ends, but also occurs at an interior region along the filaments. The structurally restricted topography of incorporation sites raises the intriguing question of how these specific active sites are generated along the filaments. At present we have not detected any correlation between these assembly "hotspots" and any morphological features of IFs, including their interaction with other cytoskeletal polymers or membrane organelles. Future detailed studies on the incorporation sites of NF proteins will provide some clues to this issue.

We estimated the turnover half-time of NF-L in the axon at 24–36 h after plating to be 40 min. This indicates that >90% of NF-L would be replaced within 3 h. In contrast, we observed a rather small portion of IFs to incorporate biotin-labeled NF-L in the axon 3 h after injection. There may be two possible explanations for this seeming discrepancy. First, injected NF-L which was first localized in the cell body might be in a transport-incompetent form, possibly due to the lack or excess of phosphorylation. Conversion of these stable aggregates into a more dynamic form would be a slow process and work as a rate-limiting step for the incorporation into the axon. Alternatively, it is also possible that the observed discrepancy is due to different de-

velopmental states of neurons analyzed by photobleaching and immunoelectron microscopy against biotin. Namely, we used neurons at 24–36 h after plating for photobleaching and at 36–58 h after plating for immunoelectron microscopy. This difference is inevitable from the point of view of the experimental design, because the introduction of sufficient fluorescent probes is difficult for neurons with longer neurites, and the introduction of biotin probes into neurons before neurite extension results in incorporation of biotin-labeled NF-L into all IFs in the growing neurites. In fact, our preliminary photobleaching experiments on more mature axons showed progressive stabilization of NFs, suggesting the possible effects of the developmental stage on the discrepancy between the two experimental approaches.

Mechanism of Net Increase of Neuronal IF Structure during Axonal Growth

The stationary nature of the photobleached zone and the fact that there is no bulk movement of biotin-NF-L containing filaments into the proximal part of the axon suggest that IF arrays in regenerating mouse DRG axons do not move en bloc. Because the photobleached zone recovered fluorescence gradually and IFs containing biotin-labeled NF-L in the axon were colocalized with unlabeled filaments, turnover and net increase of IFs in the mouse DRG axon would occur on a single filament level. Two possible mechanisms of the turnover can be considered. One is the transport of individual filaments along the axon (Lasek, 1986) and possible annealing of these filaments into pre-existing filaments. Although this mechanism could explain a large part of our present results, the progressive elongation of numerous discrete incorporation sites of biotin-labeled NF-L is rather difficult to conceptualize without assuming that the transport filaments are very short and discrete hot spots along preexisting filaments incorporate these small fragments repeatedly. However, this notion of the very short transporting filaments ultimately leads to the idea indistinguishable from the hypothesis that soluble oligomers of IFs are the unit of transport and are incorporated into pre-existing IF arrays, which is actually the second possible explanation of our data. In this case, soluble oligomers of IFs are actively transported by some unknown mechanisms into the axon and formation of new IF structure at the tip of the growing axon, which was shown directly in Fig. 6, would be explained by either new nucleation of IFs from soluble subunits or assembly from the distal ends of pre-existing filaments. Indeed, there is increasing evidence to support the idea of subunit exchange between soluble pools of IF subunits and IF polymers. In vitro fluorescence-energy transfer studies on a labeled NF-L protein and a GFAP protein (Angelides, 1989; Nakamura, 1991) supported this idea and the existence of a small, but functional pool of soluble subunits. Although previous biochemical studies have shown that the unpolymerized pool of NF is rather small in mature axons (Morris and Lasek, 1982; Black et al., 1986), the presence of this pool which exchanges subunits very actively with the polymer pool at discrete sites on individual filaments could explain a major portion of our present data. Furthermore, the hypothesis of soluble oligomer transport fits with our structural data on the organization of NFs in the axon in situ (Hirokawa, 1982; Hirokawa et al., 1984).

The precise molecular form of a functional soluble subunit is not yet clear. Our previous in vitro experiments on the molecular architecture of NFs suggested that both a 70 nm length rod, possibly a tetramer, and a pair of these rods can work as a building block of NFs by assembly at the end of unraveled filaments (Hisanaga and Hirokawa, 1990). Further experiments will be required to determine whether these 70-nm length rods and pairs of rods are functional units in vivo.

Is generalization of the proposed mechanism of NF turnover in mouse DRG neurons to other systems, especially to the axonal transport of NFs in mature axons in vivo, warranted? One possible drawback of the system we employed in this study was that mouse DRG neurons might lack the system of active transport of cytoskeletal proteins. This argument stems from the observation that the stationary nature of MTs in mouse DRG neurons strikingly contrasts with the en bloc MT movement in embryonal *Xenopus* neurons (Reinsch et al., 1991; Okabe and Hirokawa, 1992). To clarify this point, we recently characterized the behavior of both neurons, raising the possibility that the rapidly advancing *Xenopus* growth cone drags the whole axonal structure including MTs anterogradely (Okabe and Hirokawa, 1992). Furthermore, the ability of mouse DRG neurons to extend neurites longer than 2–3 mm in culture strongly suggests the presence of active transport machinery, because theoretical considerations have argued that transport of cytoskeletal proteins only by diffusion would not work if the neurite length exceeds 1 mm. Therefore, at present, we think that there is no reason to suspect the mouse DRG neurons to represent an appropriate model system for neurite growth and slow axonal transport.

Growth-dependent Regulation of Neuronal IF Dynamics

We observed differences in the rate of recovery of bleached zones in axons of different modes of growth. Because growing axons turned over IFs more rapidly, it is likely that neurons have a mechanism which precisely controls the exchanging rate of IFs (Glass and Griffin, 1991). One possible mechanism of the growth-dependent regulation of IF-turnover is the phosphorylation of neurofilament triplet proteins. Previous studies have shown that neurofilament proteins can be phosphorylated by several kinases in vitro (Hisanaga et al., 1990; Guan et al., 1992), and phosphorylation by cAMP-dependent protein kinase or protein kinase C at the amino-terminal domain can both inhibit the assembly process of NFs and induce disassembly of pre-existing filaments (Hisanaga et al., 1990). Studies on the phosphorylation state of NFs in vivo have also suggested a possible role of carboxy-terminal domain phosphorylation in the transport rate of NF proteins (Nixon and Sihag, 1991). Interestingly, extensive phosphorylation at the carboxy-terminal domain would not induce NF disassembly, because carboxy-terminal domain phosphorylation occurs on the assembled NFs along the axon (Nixon and Lewis, 1986; Sihag and Nixon, 1990). In this sense, it would be intriguing to study the types of protein kinases which are specifically activated during the stages of rapid axonal growth of DRG neurons.

On the other hand, the progressive increase of NF-M or NF-H proteins in the NF polymers may regulate the turnover. Immunocytochemical analysis of developing neurons has revealed the sequential onset of NF-L, M and H expres-

sion during neuronal maturation (Shaw and Weber, 1981; Pochter and Liem, 1984), emphasizing the possible role of NF-M and NF-H in adding stability to the NF structure. We confirmed that adult mouse DRG neurons in culture expressed all of the NF triplet proteins and that they are distributed in a similar fashion. However, immunofluorescence microscopy is far from quantitative, and it is entirely possible that the molar ratio of NF triplet proteins in each filament is precisely regulated to confer the differential stability.

The combination of the two experimental efforts of photobleaching and biotin-mediated immunocytochemistry has revealed continuous turnover of neuronal IFs within a local region of the axoplasm possibly by the mechanism of subunit exchange at numerous discrete sites on each filament. Further studies on this system and other neuronal systems by similar experimental approaches should help to elucidate the role of dynamic subunit exchange of neuronal IFs on the development and plasticity of the neuronal shape.

This work was supported by a Special Grant-in-Aid for Scientific Research from the Ministry of Education, Science and Culture of Japan, and grants from RIKEN (to N. Hirokawa).

Received for publication 30 September 1992 and in revised form 7 January 1993.

References

Albers, K., and E. Fuchs. 1987. The expression of mutant epidermal keratin cDNAs transfected in simple epithelial and squamous cell carcinoma lines. *J. Cell Biol.* 105:791–806.

Angelides, K. J., K. E. Smith, and M. Takeda. 1989. Assembly and exchange of intermediate filament proteins of neurons: neurofilaments are dynamic structures. *J. Cell Biol.* 108:1495–1506.

Black, M. M., P. Keyser, and E. Sobel. 1986. Interval between the synthesis and assembly of cytoskeletal proteins in cultured neurons. *J. Neurosci.* 6:1004–1012.

Chin, S. S. M., and R. K. H. Liem. 1989. Expression of rat neurofilament proteins NF-L and NF-M in transfected non-neuronal cells. *Eur. J. Cell Biol.* 50:475–490.

Franke, W. W. 1987. Nuclear lamins and cytoplasmic intermediate filaments: a growing multigene family. *Cell.* 48:3–4.

Geisler, N., and K. Weber. 1981. Self-assembly in vitro of the 68,000 molecular weight component of the mammalian neurofilament triplet proteins into intermediate-sized filaments. *J. Mol. Biol.* 151:565–571.

Geisler, N., U. Plessman, and K. Weber. 1985. The complete amino acid sequence of the major mammalian neurofilament protein (NF-L). *FEBS (Fed. Eur. Biochem. Soc.) Lett.* 182:475–478.

Glass, J. D., and J. W. Griffin. 1991. Neurofilament redistribution in transected nerves: evidence for bidirectional transport of neurofilaments. *J. Neurosci.* 11:3146–3154.

Gorbsky, G. J., P. J. Sammak, and G. G. Borisy. 1988. Microtubule dynamics and chromosome motion visualized in living anaphase cells. *J. Cell Biol.* 106:1185–1192.

Guan, R. J., F. L. Hall, and J. A. Cohlberg. 1992. Proline-directed protein kinase ($p34^{cdc2}/p58^{cyclin\ A}$) phosphorylates bovine neurofilaments. *J. Neurochem.* 58:1365–1371.

Hirokawa, N. 1982. The crosslinker system between neurofilaments, microtubules and membranous organelles in frog axons revealed by quick-freeze, freeze-fracture, deep-etching method. *J. Cell Biol.* 94:129–142.

Hirokawa, N. 1991. Molecular architecture and dynamics of the neuronal cytoskeleton. *In* Neuronal Cytoskeleton. R. D. Burgoyne, editor, Wiley Liss, Inc., New York. 5–74.

Hirokawa, N., M. A. Glicksman, and M. B. Willard. 1984. Organization of mammalian neurofilament polypeptides within the neuronal cytoskeleton. *J. Cell Biol.* 98:1523–1536.

Hisanaga, S., and N. Hirokawa. 1988. Structure of the peripheral domains of neurofilaments revealed by low angle rotary shadowing. *J. Mol. Biol.* 202:297–305.

Hisanaga, S., and N. Hirokawa. 1990. Molecular architecture of the neurofilament 2. Reassembly process of neurofilament L protein in vitro. *J. Mol. Biol.* 211:871–882.

Hisanaga, S., Y. Gonda, M. Inagaki, A. Ikai, and N. Hirokawa. 1990. Effects of phosphorylation of the neurofilament L protein on filamentous structures. *Cell Regul.* 1:237–248.

Hoffman, P. N., and R. J. Lasek. 1975. The slow component of axonal transport. Identification of major structural polypeptides of the axon and their generality among mammalian neurons. *J. Cell Biol.* 66:351–366.

Hollenbeck, P. J. 1989. The transport and assembly of the axonal cytoskeleton. *J. Cell Biol.* 108:223–227.

Lasek, R. J. 1986. Polymer sliding in axons. *J. Cell Sci. Suppl.* 5:161–179.

Lawson, S. N., A. A. Harper, E. I. Harper, J. A. Garson, and B. H. Anderton. 1984. A monoclonal antibody against neurofilament protein specifically labels a subpopulation of rat sensory neurons. *J. Comp. Neurol.* 228:268–272.

Lewis, S., and N. J. Cowan. 1985. Genetics, evolution, and expression of the 68,000-mol-wt neurofilament protein: isolation of a cloned cDNA probe. *J. Cell Biol.* 100:843–850.

Lim, S. S., K. J. Edson, P. C. Letourneau, and G. G. Borisy. 1990. A test of microtubule translocation during neurite elongation. *J. Cell Biol.* 111:123–130.

Lu, X., and E. B. Lane. 1990. Retrovirus-mediated transgenic keratin expression in cultured fibroblasts: specific domain functions in keratin stabilization and filament formation. *Cell.* 62:681–696.

McCormick, M. B., P. A. Coulombe, and E. Fuchs. 1990. Sorting out of keratin networks: consequences of domain swapping on IF recognition and assembly. *J. Cell Biol.* 113:1111–1124.

Miller, R. K., K. Vikstrom, and R. D. Goldman. 1991. Keratin incorporation into intermediate filament networks is a rapid process. *J. Cell Biol.* 113:843–855.

Mitchison, T. J. 1989. Polewards microtubule flux in the mitotic spindle: evidence from photoactivation of fluorescence. *J. Cell Biol.* 109:637–652.

Monteiro, M. J., and D. W. Cleveland. 1989. Expression of NF-L and NF-M in fibroblasts reveals coassembly of neurofilament and vimentin subunits. *J. Cell Biol.* 108:579–593.

Morris, J. R., and R. J. Lasek. 1982. Stable polymers of the axonal cytoskeleton. The axoplasmic ghost. *J. Cell Biol.* 92:192–198.

Nakamura, Y., M. Takeda, K. J. Angelides, K. Tada, S. Hariguchi, and T. Nishimura. 1991. Assembly, disassembly, and exchange of glial fibrillary acidic protein. *Glia.* 4:104–110.

Ngai, J., T. R. Coleman, and E. Lazarides. 1990. Localization of newly synthesized vimentin subunits reveals a novel mechanism of intermediate filament assembly. *Cell.* 60:415–427.

Nixon, R. A., and S. E. Lewis. 1986. Differential turnover of phosphate groups on neurofilament subunits in mammalian neurons in vivo. *J. Biol. Chem.* 261:16298–16301.

Nixon, R. A., and R. K. Sihag. 1991. Neurofilament phosphorylation: a new look at regulation and function. *Trends Neurosci.* 14:501–506.

Nixon, R. A. 1992. Slow axonal transport. *Curr. Opin. Cell Biol.* 4:8–14.

Okabe, S., and N. Hirokawa. 1988. Microtubule dynamics in nerve cells: analysis using microinjection of biotinylated tubulin into PC12 cells. *J. Cell Biol.* 107:651–664.

Okabe, S., and N. Hirokawa. 1989. Axonal transport. *Curr. Opin. Cell Biol.* 1:91–97.

Okabe, S., and N. Hirokawa. 1990. Turnover of fluorescently labelled tubulin and actin in the axon. *Nature (Lond.).* 343:479–482.

Okabe, S., and N. Hirokawa. 1991. Actin dynamics in growth cones. *J. Neurosci.* 11:1918–1929.

Okabe, S., and N. Hirokawa. 1992. Differential behavior of photoactivated microtubules in growing axons of mouse and frog neurons. *J. Cell Biol.* 117:105–120.

Okabe, S., and N. Hirokawa. 1993. Do photobleached fluorescent microtubules move? Re-evaluation of fluorescence laser photobleaching both in vitro and in growing *Xenopus* axon. *J. Cell Biol.* In press.

Pachter, J. S., and R. K. H. Liem. 1984. The differential appearance of neurofilament triplet proteins in the developing rat optic nerve. *Dev. Biol.* 103:200–210.

Parysek, L. M., and R. D. Goldman. 1988. Distribution of a novel 57 kDa intermediate filament (IF) protein in the nervous system. *J. Neurosci.* 8:555–563.

Reinsch, S. S., T. J. Mitchison, and M. W. Kirschner. 1991. Microtubule polymer assembly and transport during axonal elongation. *J. Cell Biol.* 115: 365–379.

Schlaepfer, W. W., and R. G. Lynch. 1977. Immunofluorescence studies of neurofilaments in rat and human peripheral and central nervous system. *J. Cell Biol.* 74:241–250.

Shaw, G., and K. Weber. 1981. The distribution of the neurofilament triplet proteins within individual neurons. *Exp. Cell Res.* 136:119–125.

Shaw, G., and K. Weber. 1981. Differential expression of neurofilament triplet proteins in brain development. *Nature (Lond.).* 298:277–279.

Sihag, R. K., and R. A. Nixon. 1990. Phosphorylation of the amino-terminal head domain of the middle molecular mass 145-kDa subunit of neurofilaments: evidence for regulation by second messenger-dependent protein kinases. *J. Biol. Chem.* 265:4166–4171.

Soellner, P., R. Quinlan, and W. W. Franke. 1985. Identification of a distinct soluble subunit of an intermediate filament protein: tetrameric vimentin from living cells. *Proc. Natl. Acad. Sci. USA.* 82:7929–7933.

Steinert, P. M., A. C. Steven, and D. R. Roop. 1985. The molecular biology of intermediate filaments. *Cell.* 42:411–419.

Tsien, R. Y. 1989. Fluorescent indicators of ion concentrations. *Methods Cell Biol.* 30:127–156.

Vigers, G. P. A., M. Coue, and J. R. McIntosh. 1988. Fluorescent microtubules break up under illumination. *J. Cell Biol.* 107:1011–1024.

Vikstrom, K. L., G. G. Borisy, and R. D. Goldman. 1989. Dynamic aspects of intermediate filament networks in BHK-21 cells. *Proc. Natl. Acad. Sci. USA.* 86:549–553.

Wang, P. C., and D. W. Cleveland. 1990. Characterization of dominant and recessive assembly-defective mutations in mouse neurofilament NF-M. *J. Cell Biol.* 111:1987–2003.